Reaction-diffusion processes in scale-free networks

Michele Catanzaro, Marián Boguñá, and Romualdo Pastor-Satorras

Abstract In this chapter we provide a review of the main results recently obtained in the modeling of binary fermionic reaction-diffusion processes on scale-free networks. We show how to derive rate equations within the heterogeneous mean-field formalism, and how information can be obtained from them both for finite networks in the diffusion-limited regime and in the infinite network size lime. By means of extensive numerical simulations, we check the mean field predictions and explore other aspects of the reaction-diffusion dynamics, such as density correlations and the effects of the minimum degree or a tree-like topology.

1 Introduction

Complex networks theory has proved in recent years to be an extremely useful tool for the study and characterization of the structure and function of many complex systems [1, 2, 3]. In fact, many natural and man-made systems have a heterogenous pattern of connexions and interactions that can be properly described as a network or graph [4]. The statistical analysis of their topological organization has shown that most of them seem to share some typical features, the most relevant being the small-world property [5] and a large heterogeneity in the number of contacts per vertex (or degree), which lacks any typical degree-scale [6].

Michele Catanzaro
Departament de Física i Enginyeria Nuclear, Universitat Politècnica de Catalunya, 08034 Barcelona, Spain

Marián Boguñá
Departament de Física Fonamental, Universitat de Barcelona, 08028 Barcelona, Spain

Romualdo Pastor-Satorras
Departament de Física i Enginyeria Nuclear, Universitat Politècnica de Catalunya, 08034 Barcelona, Spain

The small-world property refers to the fact that the average distance $\langle \ell \rangle$ between any two vertices –measured as the smallest number of connections (or edges) between them– is very small, scaling logarithmically or even slower with the network size N. This is to be compared to the polynomial scaling of $\langle \ell \rangle \sim N^{1/d}$ in a d-dimensional lattice. Since the logarithm function grows slower than any polynomial, even if $d = \infty$, small-world networks can be thought of as highly compact objects of infinite dimensionality. As a consequence, the metric properties of this class of systems are nearly absent, every vertex being roughly at the same distance to any other vertex of the network, and fluctuations associated to "spatial" effects can be neglected. This accounts for the accuracy of mean-field theories applied to the understanding of dynamical processes taking place in small-world networks [7].

On the other hand, real complex networks are not just small-worlds but also scale-free (SF) networks. They are typically characterized by a degree distribution $P(k)$ –the probability that a randomly selected vertex has degree k– that decreases as a power-law,

$$P(k) \sim k^{-\gamma}, \tag{1}$$

where γ is a characteristic degree exponent, usually in the range $2 < \gamma \leq 3$. Within this domain the topological fluctuations of the degree, characterized by its second moment $\langle k^2 \rangle$, diverge in the limit of large network sizes. It is the conjunction of the small-world and SF properties that makes complex networks radically different from more regular structures embedded in metric spaces.

Initially, the interest in networked systems was concentrated on the description and modeling of their structural properties [1, 2]. More recently, research efforts have placed the focus on the effects that these peculiar topological properties may have on the behavior of dynamical systems running on top of networks [7]. Besides their obvious theoretical interest, these efforts can have practical implications in real world systems, e.g., understanding traffic behavior in technological systems such as the Internet [8] or epidemic spreading of sexually transmitted diseases in human populations [9]. Interest in dynamics was triggered by the observation that the heterogeneous connectivity pattern observed in SF networks with diverging degree fluctuations can lead to very surprising outcomes, such as an extreme weakness in front of targeted attacks aimed at destroying the most connected vertices [10, 11], or the ease of propagation of infective agents [12, 13]. These properties are due to the critical interplay between topology and dynamics in heterogeneous networks and are absent in their homogeneous counterparts. After those initial discoveries, a real avalanche of new results have been put forward; for a summary of them we refer the reader to Ref. [7].

The importance of dynamical process on complex networks justifies the pursuit of common frameworks to describe and analyze them in a general way. One of them is the theory of reaction-diffusion (RD) processes , that can be used to represent a wide spectrum of different dynamics. In very general terms, RD processes are dynamic systems that involve particles of different "species" (A_i, $i = 1, \ldots n$) that diffuse stochastically and interact among them following a fixed set of reaction rules. In this kind of processes, the interest is usually focused on the time evolution

and steady states of the densities of the different species $\rho_{A_i}(t)$, and on the possible presence of phase transitions between those states [15].

Epidemic models, such as the Susceptible-Infected-Susceptible (SIS) [16], represent classical examples of RD dynamics. The SIS model, for instance, corresponds to a RD process with two species of particles (individuals), infected I and susceptible S, that interact through the reactions [16, 17]

$$\begin{array}{rcl} S+I & \xrightarrow{\delta} & 2I, \\ I & \xrightarrow{\mu} & S. \end{array} \tag{2}$$

The first reaction in Eq. (2) corresponds to the infection of a susceptible individual by contact with an infected one, with a probability per unit of time (rate) δ. The second reaction stands for the spontaneous healing of infected individuals at rate μ. The behavior of this epidemic model is ruled by the ratio $\lambda = \delta/\mu$, the so-called spreading rate. The main prediction of the model is the existence of an epidemic threshold λ_c, above which the dynamics reaches an endemic state, with a nonzero density of infected individuals ρ_I [17]. Below the threshold, on the other hand, any epidemics dies out in the long term, and the systems is disease-free.

Much is known about the behavior of RD processes on regular homogeneous lattices. In particular, theoretical formalisms have been proposed that allow for general descriptions of the process in terms of field theories [18, 19, 20, 21] which are then susceptible of analysis by means of the renormalization group technique [22]. For example, for the simplest RD process, the diffusion-annihilation process [23]

$$A+A \xrightarrow{\lambda} \emptyset \tag{3}$$

in regular lattices of Euclidean dimension d, it is well known that the local density of A particles, $\rho(x,t)$, is ruled by a Langevin equation [24],

$$\frac{\partial \rho(x,t)}{\partial t} = D\nabla^2 \rho(x,t) - 2\lambda \rho(x,t)^2 + \eta(x,t), \tag{4}$$

where $\eta(x,t)$ is a Gaussian white noise, with correlations

$$\langle \eta(x,t)\eta(x',t')\rangle = -2\lambda\rho(x,t)^2 \delta^d(x-x')\delta(t-t'). \tag{5}$$

Dynamical renormalization group arguments show that the average density of A particles, $\rho(t) = \langle \rho(x,t)\rangle$, behaves in the large time limit as

$$\frac{1}{\rho(t)} - \frac{1}{\rho_0} \sim t^{\alpha}, \tag{6}$$

where ρ_0 is the initial particle density, and the exponent α takes the values $\alpha = d/d_c$ for $d \leq d_c$ and $\alpha = 1$ for $d > d_c$, where $d_c = 2$ is the critical dimension of the process. For $d > d_c$ one thus recovers the homogeneous mean-field solution

$$\rho(t) \sim t^{-1}, \tag{7}$$

obtained from Eq. (4) by setting the diffusion coefficient D and the noise term $\eta(x,t)$ equal to zero.

When the substrate is not a regular lattice but a complex network with the properties described above, the powerful machinery of the renormalization group becomes incapable of solving the problem. The reason is rooted in the small-world property and the lack of a metric structure that renders the very concept of renormalization meaningless. We can then say that, in comparison, the study of the interplay of RD processes with the heterogeneous topology of a complex network is still in its infancy.

RD processes in complex networks are usually defined within a "fermionic" point of view, in which each vertex can hold at most one particle. Diffusion and dynamics are thus coupled, in the sense that particles perform random jumps between adjacent vertices and react upon landing on an already occupied vertex. This formalism has been applied, both theoretically and numerically, to the case of binary diffusion-annihilation processes with a single species $A+A \to \emptyset$ [25, 26] and with two species $A+B \to \emptyset$ [25, 27]. From the study of those systems, it has been already possible to shed some light on RD dynamics, which turns out to have an unexpected and interesting behavior when the substrate network is SF with an exponent $2 < \gamma \leq 3$. The long term dynamics, for instance, is always faster than in lattices, with the exponent $\alpha > 1$. Besides, the dynamics evolves in a hierarchical fashion, with the concentration of particles first decaying at low degree vertices, then at higher degree vertices and so on until the concentration of particles in the vertices with the maximum degree starts decreasing. Another striking difference as compared to lattices is the absence of depletion zones in the $A+A \to \emptyset$ process and the lack of segregation between species in the $A+B \to \emptyset$ one which, again, is a consequence of the small-world property.

In this chapter we provide a review of the main results obtained in the modeling of binary fermionic RD processes in SF networks. We have organized it as follows: in section 2 we summarize the standard analytical technique used to deal with dynamical processes on complex networks, namely heterogeneous mean-field (MF) theory. Applied to the case of RD processes, we focus on a general process that encompasses both $A+A \to \emptyset$ and $A+B \to \emptyset$ as particular cases. We show the general procedure to obtain a MF rate equation for the particle density, and how to solve it both in finite networks (within the so-called diffusion-limited regime) and in the infinite network size limit, by means of a continuous degree approximation. Section 3 is devoted to show the results than can be obtained by means of numerical Monte Carlo simulations. After checking the analytical predictions of MF theory, we consider other aspects numerically observed in this kind of systems: the lack of depletion and segregation effects, which can be related to the density correlations of particles; the role of the degree in the annihilation dynamics; the effects of the minimum degree of the network substrate; and the effects of global constraints, such as the absence of loops (tree topologies). Finally, in section 4 we present an outlook of the future venues of research in the field of RD processes in complex networks.

2 Analytical description of diffusion-annihilation processes in complex networks

Let us consider the most general two species diffusion-annihilation process, given by particles of two species A and B, and that is defined by the reaction rules

$$\begin{aligned} A+A &\to \emptyset \quad \text{with probability } p_{aa} \\ A+B &\to \emptyset \quad \text{with probability } p_{ab} \\ B+B &\to \emptyset \quad \text{with probability } p_{bb}. \end{aligned} \tag{8}$$

The processes take place on an arbitrary complex network of size N, each vertex of which can host at most one particle. The dynamics of the process is defined as follows: At rate λ, an A particle chooses one of its nearest neighbor. If it is empty, the particle fills it, leaving the first vertex empty. If the nearest neighbor is occupied by another A particle, the two particles annihilate with probability p_{aa}, leaving both vertices empty. If the nearest neighbor is occupied by a B particle, both particles annihilate with probability p_{ab}. If the annihilation events do not take place, all particles remain in their original positions. The same dynamics applies to B particles if we replace p_{aa} by p_{bb}. We also assume that the diffusion rate λ is the same for both types of particles. It is easy to see that, with this formulation, $p_{aa} = p_{bb} = p_{ab} = 1$ corresponds to the $A+A \to \emptyset$ process since, in this case, there is no way to distinguish between A and B particles. On the contrary, setting $p_{aa} = p_{bb} = 0$ and $p_{ab} = 1$, one recovers the $A+B \to \emptyset$ process.

2.1 Heterogeneous mean-field formalism

The inherent randomness in the topology of complex networks forces us to describe them using a statistical framework. In this chapter, we consider the simplest statistical description of a network in terms of the properties of single vertices (degrees) and correlations between pairs of such vertices, the so-called degree-degree correlations. Single vertex statistical properties are encoded in the degree distribution $P(k)$ and degree-degree correlations are described by the conditional probability $P(k'|k)$ that a vertex of degree k is connected to a vertex of degree k' [28]. We should note that all the results presented here are correct for networks maximally random –in the sense of maximizing the entropy of the network– under the constraints of having given functions $P(k)$ and $P(k'|k)$. Once this assumption is done, we can get some analytical insights on the behavior of diffusion-annihilation processes by applying the heterogeneous MF theory –a mean-field description of the dynamics that discriminates between degree classes [26, 27].

To study analytically this process within this approximation, we are forced to consider the partial densities $\rho_k^a(t)$ and $\rho_k^b(t)$, representing the density of A and B

particles in vertices of degree k, or, in other words, the probabilities that a vertex of degree k contains an A or B particle at time t [12, 29]. From these partial densities, the total densities of A and B particles are recovered from

$$\rho^a(t) = \sum_k P(k)\rho_k^a(t) \qquad \text{and} \qquad \rho^b(t) = \sum_k P(k)\rho_k^b(t). \tag{9}$$

While it is possible to obtain rate equations for the densities $\rho_k^a(t)$ and $\rho_k^b(t)$ by means of intuitive arguments [12, 30], in the following we will pursue a more microscopical approach [26], which can be generalized to tackle other kind of problems.

Let us consider the process defined in Eq. (8) on a network of N vertices which is fully defined by its adjacency matrix a_{ij}, taking the values $a_{ij} = 1$ if vertices i and j are connected by an edge and 0 otherwise. Let $n_i^a(t)$ be a dichotomous random variable taking value 1 whenever vertex i is occupied by an A particle and 0 otherwise. Analogously, let $n_i^b(t)$ be a dichotomous random variable taking value 1 whenever vertex i is occupied by a B particle and 0 otherwise. Notice that with the previous definition, the random variable $1 - n_i^a(t) - n_i^b(t)$ takes the value 1 when vertex i is empty and is zero in any other situation, so that it defines the complementary event of being occupied by an A or B particle. This property assures the correct fermionic description of the dynamics. The state of the system at time t is completely defined by the state vectors $\mathbf{n}^a(t) = \{n_1^a(t), n_2^a(t), \cdots, n_N^a(t)\}$ and $\mathbf{n}^b(t) = \{n_1^b(t), n_2^b(t), \cdots, n_N^b(t)\}$, denoted for simplicity $\mathbf{n}(t) \equiv (\mathbf{n}^a(t), \mathbf{n}^b(t))$. Assuming that diffusion and annihilation events of the particles follow independent Poisson processes [14], the evolution of $\mathbf{n}(t)$ after a time increment dt can be expressed as

$$n_i^a(t+dt) = n_i^a(t)\eta(dt) + [1 - n_i^a(t) - n_i^b(t)]\xi(dt), \tag{10}$$

with an analogous equation for the occupancy of B particles, n_i^b. Notice that the two terms in the r. h. s. of Eq. (10) cannot be different from zero simultaneously since they represent events that exclude each other –either vertex i holds an A particle (the first term) or it does not (the second one). In this way, the evolution at time $t + dt$ is tied to the state of the system at the previous time t.

The variables $\eta(dt)$ and $\xi(dt)$ in Eq. (10) are dichotomous random variables taking values

$$\eta(dt) = \begin{cases} 0 \;\text{ with prob. }\; \lambda\, dt \left[1 - \displaystyle\sum_j \frac{a_{ij}[(1-p_{aa})n_j^a(t) + (1-p_{ab})n_j^b(t)]}{k_i} \right. \\ \qquad\qquad\qquad\qquad \left. + \displaystyle\sum_j \frac{a_{ij}[p_{aa}n_j^a(t) + p_{ab}n_j^b(t)]}{k_j} \right] \\ 1 \;\text{ otherwise} \end{cases}, \tag{11}$$

and

$$\xi(dt) = \begin{cases} 1 \text{ with prob. } \lambda dt \sum_j \dfrac{a_{ij} n_j^a(t)}{k_j} \\ 0 \text{ otherwise} \end{cases} , \tag{12}$$

where λ is the jumping rate that, without loss of generality, we set equal to 1. The first term in Eq. (10) stands for an event in which vertex i is occupied by an A particle and, during the time interval $(t, t+dt)$, it becomes empty either because the particle in it decides to move to another empty vertex or because it annihilates with one of its nearby A or B particles. The second term corresponds to the case in which vertex i is empty and an A particle in a neighboring vertex of i decides to move to that vertex[1]. Taking the average of Eq. (10), we obtain

$$\begin{aligned} \langle n_i^a(t+dt) | \mathbf{n}(t) \rangle = n_i^a(t) \\ - \left[-\sum_j \frac{a_{ij}[(1-p_{aa}) n_i^a(t) n_j^a(t) + (1-p_{ab}) n_i^a(t) n_j^b(t)]}{k_i} \right. \\ \left. + n_i^a(t) + \sum_j \frac{a_{ij}[p_{aa} n_i^a(t) n_j^a(t) + p_{ab} n_i^a(t) n_j^b(t)]}{k_j} \right] dt \\ + [1 - n_i^a(t) - n_i^b(t)] \sum_j \frac{a_{ij} n_j^a(t)}{k_j} dt, \end{aligned} \tag{13}$$

equation that describes the average evolution of the system, conditioned to the knowledge of its state at the previous time step. Then, after multiplying Eq. (13) by the probability to find the system at state $\mathbf{n}$ at time t, and summing for all possible configurations, we are led to

$$\begin{aligned} \frac{d\rho_i^a(t)}{dt} = -\rho_i^a(t) + \sum_j \frac{a_{ij}[(1-p_{aa}) \rho_{ij}^{aa}(t) + (1-p_{ab}) \rho_{ij}^{ab}(t)]}{k_i} \\ - \sum_j \frac{a_{ij}[p_{aa} \rho_{ij}^{aa}(t) + p_{ab} \rho_{ij}^{ab}(t)]}{k_j} + \sum_j \frac{a_{ij}[\rho_j^a(t) - \rho_{ij}^{aa}(t) - \rho_{ij}^{ba}(t)]}{k_j}, \end{aligned} \tag{14}$$

where we have introduced the notation

$$\rho_i^a(t) \equiv \langle n_i^a(t) \rangle \quad , \quad \rho_i^b(t) \equiv \langle n_i^b(t) \rangle, \tag{15}$$

$$\rho_{ij}^{aa}(t) \equiv \langle n_i^a(t) n_j^a(t) \rangle \quad \text{and} \quad \rho_{ij}^{ab}(t) \equiv \langle n_i^a(t) n_j^b(t) \rangle. \tag{16}$$

Notice that $\rho_{ij}^{ab}(t) \neq \rho_{ij}^{ba}(t)$.

[1] Notice that the random variables $\eta(dt)$ and $\xi(dt)$ are not independent, since both involve some common random movements. This fact, however, does not affect the mean-field analysis, which do not involve cross correlations between them.

The derivation presented so far is exact, but difficult to deal with. However, it is possible to obtain useful information if we restrict our analysis to the class of random networks with given degree distribution and degree-degree correlations but maximally random at all other respects. For this class of networks, vertices of the same degree can be considered as statistically equivalent. In mathematical terms, this means that [30]

$$\rho_i^a(t) \equiv \rho_k^a(t) \qquad \forall i \in \mathscr{V}(k), \tag{17}$$
$$\rho_i^b(t) \equiv \rho_k^b(t) \qquad \forall i \in \mathscr{V}(k), \tag{18}$$
$$\rho_{ij}^{aa}(t) \equiv \rho_{kk'}^{aa}(t) \qquad \forall i \in \mathscr{V}(k),\ j \in \mathscr{V}(k') \tag{19}$$
$$\rho_{ij}^{ab}(t) \equiv \rho_{kk'}^{ab}(t) \qquad \forall i \in \mathscr{V}(k),\ j \in \mathscr{V}(k'), \tag{20}$$

where $\mathscr{V}(k)$ is the set of vertices of degree k. Besides, the small world property present in this class of networks makes them objects of infinite dimensionality, well described by a MF theory. In such situation, correlations between elements can be neglected and, consequently, we can approximate two point correlations functions as $\rho_{kk'}(t) \simeq \rho_k(t)\rho_{k'}(t)$. Using these ideas in Eq. (14) we can write the following closed equation for the degree-dependent densities

$$\begin{aligned}\frac{d\rho_k^a(t)}{dt} = &- \rho_k^a(t) + \rho_k^a(t)\sum_{k'} P(k'|k)\left[(1-p_{aa})\rho_{k'}^a(t) + (1-p_{ab})\rho_{k'}^b(t)\right] \\ &- \rho_k^a(t)\sum_{k'}\frac{kP(k'|k)}{k'}\left[p_{aa}\rho_{k'}^a(t) + p_{ab}\rho_{k'}^b(t)\right] \\ &+ (1-\rho_k^a(t)-\rho_k^b(t))\sum_{k'}\frac{kP(k'|k)}{k'}\rho_{k'}^a(t),\end{aligned} \tag{21}$$

where we have made use of the identity [30]

$$\frac{1}{NP(k)}\sum_{i\in\mathscr{V}(k)}\sum_{j\in\mathscr{V}(k')} a_{ij} = kP(k'|k). \tag{22}$$

The equation for the density of B particles can be obtained from Eq. (21) by swapping indices a and b.

Eq. (21) can be further simplified if we assume that A and B particles react among them with the same probability, that is, $p_{aa} = p_{bb}$. In this case (and assuming also the same concentration of A and B particles at $t = 0$), the total density of particles in vertices of degree k, $\rho_k(t) = \rho_k^a(t) + \rho_k^b(t)$, can be written as

$$\begin{aligned}\frac{d\rho_k(t)}{dt} = &-\rho_k(t) + (1-\mu)\rho_k(t)\sum_{k'} P(k'|k)\rho_{k'}(t) \\ &+ [1-(1+\mu)\rho_k(t)]\sum_{k'}\frac{kP(k'|k)}{k'}\rho_{k'}(t),\end{aligned} \tag{23}$$

while the total density $\rho(t) = \sum_k P(k)\rho_k(t)$ fulfills the differential equation

$$\frac{d\rho(t)}{dt} = -2\mu \sum_k P(k)\rho_k(t)\Theta_k(t), \tag{24}$$

where we have used the degree detailed balance condition [28]

$$kP(k)P(k'|k) = k'P(k')P(k|k'). \tag{25}$$

In Eq. (24) we have defined

$$\Theta_k(t) = \sum_{k'} P(k'|k)\rho_{k'}(t) \tag{26}$$

as the probability that a randomly chosen edge in a vertex of degree k points to a vertex occupied by an A or B particle, while the parameter $\mu \in [0,1]$ is defined as $\mu = (p_{aa} + p_{ab})/2$. In this way, by setting $\mu = 1/2$ we recover the equation describing the $A+B \to \emptyset$ process [27], whereas $\mu = 1$ describes the $A+A \to \emptyset$ one [26]. It is interesting that, in this case, the model is described by a single parameter μ, even if, originally, there were two of them, p_{aa} and p_{ab}. This implies that there is a whole set of different models which are governed by the same dynamical equation.

2.2 Finite networks: Diffusion-limited regime

In the case of networks with a general pattern of degree correlations, the solution of Eq. (23) depends on the nature of the conditional probability $P(k'|k)$ and can be a rather demanding task [31]. General statements on the total density of particles can be made, however, in the limit of very long time and very small particle density, when the concentration of particles is so low that the RD process is driven essentially by diffusion. In this diffusion-limited regime, it is possible to estimate the behavior of $\rho(t)$, which turns out to be independent of the correlation pattern of the network.

If we consider Eq. (23) in the limit $\rho_k \to 0$ (i.e. at large times), linear terms dominate, and we can consider the simplified linear equation

$$\frac{d\rho_k(t)}{dt} \simeq -\rho_k(t) + \sum_{k'} \frac{kP(k'|k)}{k'}\rho_{k'}(t), \tag{27}$$

that is, the density behaves as in a pure diffusion problem. The time scale for the diffusion of the particles is much smaller than the time scale for two consecutive reaction events. Therefore, the partial density can relax to the stationary state of Eq. (27) and is well approximated by a pure diffusion of particles [32, 33]

$$\rho_k(t) \simeq \frac{k}{\langle k \rangle}\rho(t), \tag{28}$$

proportional to the degree k and the total instantaneous concentration of particles, and independent of degree correlations. Inserting this quasi-static approximation

back into the general Eq. (24), we obtain for long times and finite size networks the equation

$$\frac{d\rho(t)}{dt} \simeq -2\mu\rho(t)^2 \frac{\langle k^2\rangle}{\langle k\rangle^2}, \tag{29}$$

where $\langle k^2\rangle = \sum_k k^2 P(k)$ is the second moment of the degree distribution. The solution of this equation is

$$\frac{1}{\rho(t)} - \frac{1}{\rho_0} \simeq 2\mu \frac{\langle k^2\rangle}{\langle k\rangle^2} t, \tag{30}$$

that is, linear in t with a prefactor depending on the fluctuations of the degree. For homogeneous networks with a bounded degree distribution, $\langle k^2\rangle$ is finite, and so is the density prefactor. In SF networks, the prefactor depends on the cutoff –or maximum degree in the network– $k_c(N)$ [34], with

$$\langle k^2\rangle \sim \begin{cases} k_c(N)^{3-\gamma} & \text{for } \gamma < 3 \\ \ln k_c(N) & \text{for } \gamma = 3 \end{cases}, \tag{31}$$

which is an increasing function of the network size N. The specific functional form of k_c on N depends, in general, on the particular model under consideration. For uncorrelated SF networks, such as those created with the uncorrelated configuration model (UCM) [35], we have $k_c(N) \sim N^{1/2}$, the so-called structural cutoff [36]. For correlated networks created with the configuration model (CM) [37], we have instead a natural[2] cutoff $k_c(N) \sim N^{1/(\gamma-1)}$ [34]. Therefore, the behavior of the particle density in the diffusion-limited regime can be summarized as

$$\frac{1}{\rho(t)} \sim \begin{cases} N^{(3-\gamma)/2} t & \text{UCM, } \gamma < 3 \\ N^{(3-\gamma)/(\gamma-1)} t & \text{CM, } \gamma < 3 \\ \ln Nt & \gamma = 3 \\ t & \gamma > 3 \end{cases}. \tag{32}$$

This result implies that, for the CM model, the diffusion-limited regime is reached at lower particle concentrations as compared to the UCM. This result has been observed in numerical simulations in Ref. [38].

2.3 Infinite networks: Continuous degree approximation

As we have mentioned before, the solution of the general Eqs. (23) and (24) can be very difficult to obtain in networks with general correlations $P(k'|k)$. A completely analytical solution in the limit of infinite size networks can, however, be obtained

[2] The name "structural cutoff" refers to the fact that it is the maximum degree allowing us to built uncorrelated networks. Beyond this limit, structural degree correlations appear as a consequence of the closure of the network. Instead, "natural cutoff" refers to the expected maximum degree when we generate N independent random trials from the degree distribution $P(k)$ without actually closing the network.

in the case of uncorrelated networks, in which the conditional probability takes the simple form $P(k'|k) = k'P(k')/\langle k\rangle$ [30]. For this class of networks, the rate equation is

$$\frac{d\rho_k(t)}{dt} = -\rho_k(t) + (1-\mu)\Theta(t) + [1-(1+\mu)\rho_k(t)]\frac{k}{\langle k\rangle}\rho(t), \tag{33}$$

and

$$\frac{d\rho(t)}{dt} = -2\mu\rho(t)\Theta(t), \tag{34}$$

where we have defined

$$\Theta(t) = \frac{1}{\langle k\rangle}\sum_k kP(k)\rho_k(t). \tag{35}$$

In order to solve Eq. (33), we perform a *quasi-static* approximation. From the homogeneous MF solution of the $A+A\to\emptyset$ and $A+B\to\emptyset$ processes, we expect $\rho(t)$ to be a decreasing function with a power-law-like behavior. In this case, for large enough times, the time derivative of $\rho(t)$ will be much smaller that the density proper, that is, $\partial_t\rho(t) \ll \rho(t)$. Extending this argument to the partial densities $\rho_k(t)$, at long times we can neglect the left-hand-side term in Eq. (33), and solve for $\rho_k(t)$ as a function of the density, obtaining

$$\rho_k(t) = \frac{\dfrac{k\rho(t)}{\langle k\rangle}}{1+(1+\mu)\dfrac{k\rho(t)}{\langle k\rangle} - (1-\mu)\Theta(t)}. \tag{36}$$

Substituting this approximation into the expression for $\Theta(t)$, we get

$$\Theta(t) = \frac{1}{\langle k\rangle^2[1-(1-\mu)\Theta(t)]}\sum_k \frac{P(k)k^2\rho(t)}{1+\frac{1+\mu}{1-(1-\mu)\Theta(t)}\frac{k\rho(t)}{\langle k\rangle}}. \tag{37}$$

Solving this self-consistent equation, we can find $\Theta(t)$ as a function of $\rho(t)$, and then proceed to solve Eq. (34). For heterogenous networks with a diverging second moment, as in the case of SF networks, we have to consider carefully the solution of Eq. (37). If we consider a continuous degree approximation, uncorrelated SF networks in the infinite size limit are completely determined by the normalized degree distribution

$$P(k) = (\gamma-1)m^{\gamma-1}k^{-\gamma}, \tag{38}$$

where m is the minimum degree in the network, and we are approximating k as a continuous variable. The average degree is thus $\langle k\rangle = m(\gamma-1)/(\gamma-2)$. Within this approximation, Eq. (37) can be written as

$$\Theta(t) = \frac{(\gamma-1)m^{\gamma-1}\rho(t)}{\langle k\rangle^2[1-(1-\mu)\Theta(t)]}\int_m^\infty \frac{k^{2-\gamma}}{1+\frac{1+\mu}{1-(1-\mu)\Theta(t)}\frac{k\rho(t)}{\langle k\rangle}}dk \tag{39}$$

$$= \frac{1}{1+\mu} F\left[1, \gamma-2, \gamma-1, -\frac{\langle k\rangle[1-(1-\mu)\Theta(t)]}{m(1+\mu)\rho(t)}\right] \tag{40}$$

where $F[a,b,c,z]$ is the Gauss hypergeometric function [39]. Assuming both $\Theta(t)$ and $\rho(t)$ small (i.e. for sufficiently long times), we can use the asymptotic expansion of the Gauss hypergeometric function

$$F[1,\gamma-2,\gamma-1,-1/z] \sim \begin{cases} z^{\gamma-2} & \gamma<3 \\ -z\ln z & \gamma=3 \\ z & \gamma>3 \end{cases}, \quad \text{for } z\to 0, \tag{41}$$

to obtain and explicit expression of $\Theta(t)$ as a function of $\rho(t)$. Inserting it into the rate equation for $\rho(t)$ and integrating, we obtain the explicit solutions in the long time limit for infinite size uncorrelated SF networks

$$\frac{1}{\rho(t)} \sim \begin{cases} t^{1/(\gamma-2)} & \gamma<3 \\ t\ln t & \gamma=3 \\ t & \gamma>3 \end{cases}. \tag{42}$$

That is, apart from irrelevant prefactors, the leading solution is independent of μ, and therefore the same for both $A+A\to\emptyset$ and $A+B\to\emptyset$ processes [26, 27].

The analytical exponents derived above are exact for infinite size networks. However, they may be difficult to observe in real computer simulations performed on networks of finite size. We can see this fact from the quasi-static approximation Eq. (36), in which, for the sake of simplicity, we will focus in the case $\mu=1$ ($A+A\to\emptyset$ process). Indeed, for a power-law degree distribution, the largest weight in the sum in Eq. (37) is carried by the large k values. If the network is composed of a finite number of vertices, N, as it always happens in numerical simulations, it has a cutoff or maximum degree $k_c(N)$, Thus, there exists a cross-over time t_c, defined by

$$\frac{2k_c(N)\rho(t_c)}{\langle k\rangle} \sim 1, \tag{43}$$

such that, for $t>t_c$ the particle density is so small that we can approximate

$$\rho_k(t) \simeq \frac{k}{\langle k\rangle}\rho(t), \tag{44}$$

which corresponds to the diffusion-limited regime discussed in Section 2.2. Therefore, for $t>t_c$, we should expect to observe a linear behavior on $1/\rho(t)$, instead of the power-law predicted in infinite networks for the continuous degree approximation, while the region for the asymptotic infinite size behavior should be observed for $t<t_c$. From Eqs. (43) and (42) we can predict

$$t_c(N) \sim k_c(N)^{\gamma-2} \sim N^{(\gamma-2)/2} \tag{45}$$

for uncorrelated networks. This is an increasing function of N for $\gamma<3$ and so one should expect that the region in which the infinite size behavior is observed must

be increasing with N. However, the width of this region must be properly compared with the total surviving time of the process in a finite network. Assuming that at long times the process is dominated by the diffusion-limited regime, Eq. (32), we can estimate the total duration of the process as the time t_d at which only two particles remain, that is,

$$\rho(t_d) \sim \frac{2}{N}. \tag{46}$$

From this definition, we can estimate

$$t_d(N) \sim N^{(\gamma-1)/2}. \tag{47}$$

The ratio of the crossover time to the total duration of the process is thus

$$\frac{t_c(N)}{t_d(N)} \sim N^{-1/2}, \tag{48}$$

that is, a decreasing function of N. Therefore, the RD dynamics is dominated by its diffusion-limited regime. Consequently, even for very large systems, the asymptotic infinite size behavior will be very difficult to observe whereas the diffusion-limited regime will span almost all the observation time.

3 Numerical simulations

The general process described by the reactions (8) can be easily implemented in numerical simulations using a sequential updating algorithm [15]. An initial fraction $\rho_0 < 1$ of vertices in the networks are chosen and randomly occupied by a $\rho_0 N/2$ particles of species A and $\rho_0 N/2$ particles of species B. At time t in the simulation, a vertex is randomly chosen among the $n(t) = n_A(t) + n_B(t)$ vertices that host an A or B particle at that time. One of its neighbors is selected also at random. If it is empty, the particle moves and occupies it. If it contains a particle, both particles react according to the rules in Eq. (8) and the particle numbers $n_A(t)$ and $n_B(t)$ are updated according to the result of the reaction step. In any case, time is updated as $t \to t + 1/n(t)$.

RD simulations are run on SF networks generated using the uncorrelated configuration model (UCM) [35], which is defined as follows. 1) We first assign to each vertex i –in a set of N initially disconnected vertices– a degree k_i extracted from the probability distribution $P(k) \sim k^{-\gamma}$, and subject to the constraints $m \leq k_i \leq N^{1/2}$ and $\sum_i k_i$ even. 2) We then construct the network by randomly connecting the vertices with $\sum_i k_i/2$ edges, respecting the preassigned degrees and avoiding multiple and self-connections. Using this algorithm, it is possible to create SF networks whose cutoff scales as $k_c(N) \sim N^{1/2}$ for any degree exponent, and which are completely uncorrelated. If instead of bounding the maximum degree by $N^{1/2}$, we leave degrees unbounded (i.e.,$m \leq k_i \leq N$, like in the configuration model [40, 41, 42, 43]) and proceed to assemble the network from step 2), avoiding the creation of multiple con-

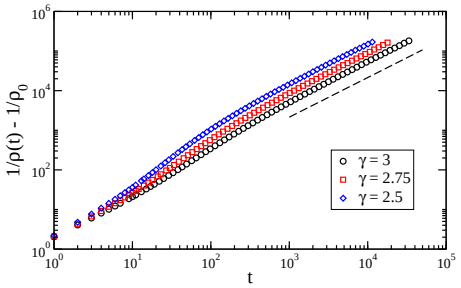

Fig. 1 Inverse average particle density $\rho(t)$ as a function of time for the $A+A \to \emptyset$ process in uncorrelated SF networks with different degree exponents and size $N = 10^6$. The dashed line corresponds to the finite size behavior $1/\rho(t) \sim t$.

nections and self-loops, the presence of very high degree vertices for $\gamma < 3$ leads to a cutoff scaling as $k_c(N) \sim N^{1/(\gamma-2)}$ and to the emergence of unavoidable structural degree-degree correlations [44, 45, 36].

From the theoretical formalism developed in Section 2, it is easy to see that the second term in the right hand side of Eq. (23) describes diffusion events that cannot take place because neighboring vertices are already occupied –when p_{aa} and p_{ab} are smaller than 1. Therefore, it describes a jamming effect that will be relevant when the concentration of particles is large, that is, at short times. However, for sufficiently long times and low concentration of particles, this jamming effect becomes weak and this term can be neglected [27]. In this situation, the dynamics becomes equivalent to the $A+A \to \emptyset$ one. For this reason, in this section we will mainly focus in the numerical results obtained for this particular case.

3.1 Density decay in uncorrelated networks

The main prediction of Section 2 is that the total density of particles should decay with time in uncorrelated networks of infinite size as predicted by Eq. (42) and as given by Eq. (32) in uncorrelated finite size networks in the diffusion-limited regime. In Fig. 1, we represent the inverse particle density from computer simulations in networks with different degree exponent γ in UCM networks. At the initial time regime, the growth of this function is faster for smaller values of the exponent γ, in agreement with the theoretical prediction Eq. (42). At longer times, on the other hand, finite size effects take over and one observes the linear regime described by Eq. (32).

The size dependence of the slope of the linear behavior in the diffusion-limited regime can also be checked using numerical simulations. In Fig. 2, one can see that, for a fixed degree exponent $\gamma = 2.5$, the curves for increasing values of N show an increase of the slope in the final linear region. Linear fits to the final part of each curve give an estimation of the increase of the slope as a function of N. We show this slope in the inset of Fig. 2, in very good agreement with the theoretical prediction Eq. (32).

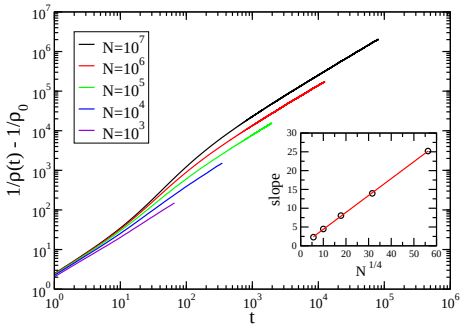

Fig. 2 Inverse average particle density $\rho(t)$ as a function of time for the $A+A \to \emptyset$ process in uncorrelated networks with degree exponent $\gamma = 2.5$ for different network sizes. Inset: slope in the linear regime as a function of N, according to the prediction in Eq. (32)

As we have discussed in section 2.3, even for the large network sizes considered in our simulations, the diffusion-limited regime takes over so quickly that it is very difficult to perform a direct quantitative check of the predicted infinite size limit regime. Using the simulation results presented in Fig. 2, we can give a rough estimate of the size of the network needed to recover the predicted behavior $\rho(t) \sim t^{-1/(\gamma-2)}$. We perform fits of the form $\rho(t) \sim t^{-\alpha_L}$ in the time window from $t \approx 10$ to just before the diffusion limited regime for the different network sizes considered. Figure 3 shows the dependence of α_L on the size of the network. The growth of α_L is extremely slow and can be well fitted by a logarithmic function. Using this fitting, we can extrapolate at which size the observed exponent would attain its theoretical value $\alpha = 1/(\gamma-2)$. For $\gamma = 2.5$, this method gives as a lower bound $N \approx 6 \times 10^9$ far beyond the computing capabilities of modern computers.

3.2 Depletion, segregation, and dynamical correlations

One of the most relevant differences between diffusion-annihilation processes on SF networks as compared to regular lattices or homogeneous networks is that in the first case the dynamics is remarkably faster, with the particle density decaying in time as a power law with an exponent larger than 1. This fact corresponds to the absence of two mechanisms that are spontaneously generated in lattices and have a slowing

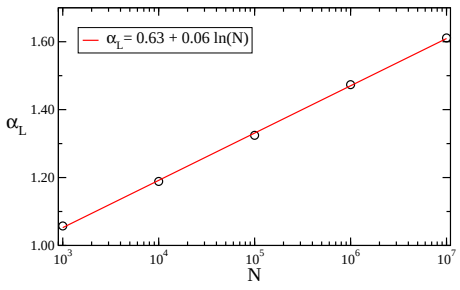

Fig. 3 Local exponent α_L as a function of the network size, obtained by fitting a power law function in the time domain before the diffusion-limited regime. Data form Fig. 2.

effect on dynamics: namely, *depletion* [46, 47] and *segregation* [48]. The first one appears in $A+A \to \emptyset$ processes: a depletion zone of empty sites is generated around any occupied site. The second takes place in $A+B \to \emptyset$ processes: a particle is typically surrounded by particles of the same type, generating an overall segregation between the two species. Since particles have to get in contact or mix in order to react, this phenomena result in a slowing down of the dynamics, characterized by a power-law decrease of the density with an exponent smaller than 1 (see Eq. (6)).

A measure to detect this phenomenon in complex networks was introduced in [25, 49]. In the case of the $A+A \to \emptyset$ process, it was proposed to measure the quantity

$$Q_{AA}(t) = \frac{N_{AA}(t)}{n(t)[n(t)-1]} \tag{49}$$

that is, the number $N_{AA}(t)$ of close contacts between particles (a close contact is defined by the existence of a link between two occupied vertices), divided by the upper bound of the number of possible contacts between existing particles. A high $Q_{AA}(t)$ score (close to 1) corresponds to a case when nearly all particles form one cluster, while a decrease of this value suggests that particles are placed apart from each other. With the same line of reasoning, for the $A+B \to \emptyset$ process one can measure [25, 50]

$$Q_{AB}(t) = \frac{N_{AB}(t)}{N_{AA}(t)+N_{BB}(t)} \tag{50}$$

that is, the number of close contacts between unlike particles compared to the number of close contacts between particles of the same type. A high $Q_{AB}(t)$ score corresponds to the case when particles of different type are mixed, while a decrease of this value suggests that particles are segregated in homogeneous groups.

These measures, however, present some inconvenients. In the first one, Eq. (49), the denominator does not take into account the specific topology of the network, and compares the number of contacts with the upper bound of the number of possible contacts (i.e. the number of possible contacts if all occupied sites were connected to each other). A proper measure should take into account the real possible contacts between particles, which is determined by the special topology of the subgraphs formed by the occupied sites. In the second case, Eq. (50), the number of connexions N_{AB} is not clearly related to $N_{AA}+N_{BB}$, yielding a quantity that could occasionally diverge.

An alternative measure to quantify depletion and segregation is the explicit calculation of the density correlations proposed in Ref. [27]. Let us consider for simplicity the $A+A \to \emptyset$ process. One can define a particle correlation function by measuring at a certain time t the average density of particles in the nearest neighbors of an occupied vertex,

$$\rho_{nn}(t) = \frac{1}{n(t)} \left\langle \sum_i n_i(t) \sum_j \frac{a_{ij} n_j(t)}{k_i} \right\rangle, \tag{51}$$

where the brackets denote a dynamical average and $n_i(t)$ is the occupation number of vertex i at time t. Comparing this quantity with the overall density $\rho(t)$, we can

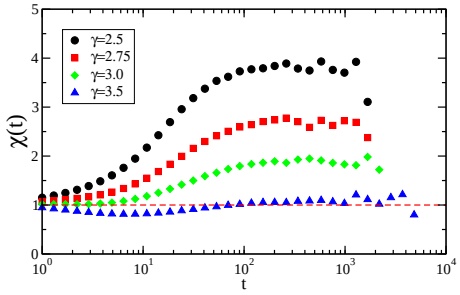

Fig. 4 Normalized density correlations for the $A+A\to\emptyset$ process as a function of time for different time snapshots. Dynamics run on uncorrelated SF networks of degree exponent $\gamma=2.5$ and size $N=10^5$.

define the normalized correlation function:

$$\chi(t)=\frac{\rho_{nn}(t)}{\rho(t)}. \tag{52}$$

When $\chi(t)$ is smaller than one, the density in the surroundings of an occupied site is smaller than the average density, which implies the presence of depletion, segregation or density anticorrelations. In the opposite case, when $\chi(t)$ is larger than one, in the neighborhood of an occupied site the particle density is larger that the average, signaling accumulation, mixing of particles or positive density correlations. The case $\chi(t)=1$ identifies lack of density correlations, in which particles are homogeneously distributed across the network substrate. Figure 4 shows simulation results of the normalized correlation functions for the $A+A\to\emptyset$ process in UCM networks. We can see that function $\chi(t)$ is larger than 1 for $\gamma\leq 3$, signaling the presence of positive correlations, or, correspondingly, the absence of depletion zones, being the surviving particles at any given time accumulated in closely connected clusters, a fact that accelerates the annihilation dynamics with respect to Euclidean lattices, in which segregation occurs. The absence of depletion is more marked for smaller values of γ, and only present at small time scales for values of $\gamma>3$.

Correlation measures can be resolved in degree, in order to yield information on the effects of the topological structure of the network, by restricting the summation in Eq. (51) to the degree class k:

$$\rho_{nn}(t;k)=\frac{1}{n_k(t)}\left\langle\sum_{i\in\mathscr{V}(k)}n_i(t)\sum_j\frac{a_{ij}n_j(t)}{k}\right\rangle, \tag{53}$$

and from which a normalized degree resolved correlation function can be defined, namely

$$\chi(t;k)=\frac{\rho_{nn}(t;k)}{\rho(t)}. \tag{54}$$

Figure 5 shows simulation results for this quantity for the $A+A\to\emptyset$ process. We can see here that the connected clusters of particles evidenced in Fig. 4 correspond to the neighborhoods of the vertices with largest degree, which show a largest value of $\chi(t;k)$.

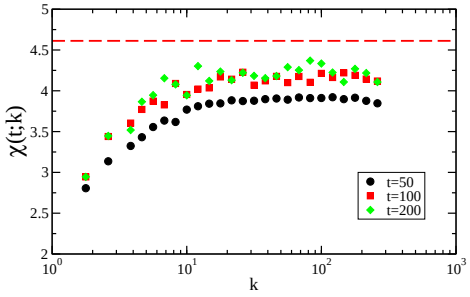

Fig. 5 Normalized density correlations for the $A+A\to\emptyset$ process as a function of time resolved in degree for different time snapshots. Dynamics run on uncorrelated SF networks of degree exponent $\gamma=2.5$ and size $N=10^5$. The dashed line marks the MF prediction for lack of dynamical correlations, Eq. (57).

The increasing values of the function $\chi(t)$ as the degree exponent γ decreases can be understood within the MF formalism. The MF approximation assumes lack of dynamical correlations between the concentration of nearby vertices. Under this approach, the density product inside the brackets can be substituted by the product of densities, yielding

$$\rho^0_{nn}(t;k) = \frac{1}{n_k(t)} \sum_{i\in\mathscr{V}(k)} \langle n_i(t)\rangle \sum_j \frac{a_{ij}\left\langle n_j(t)\right\rangle}{k} \tag{55}$$

$$= \frac{\rho_k(t)}{n_k(t)} \sum_{k'} \rho_{k'}(t) \sum_{i\in\mathscr{V}(k)} \sum_{j\in\mathscr{V}(k')} \frac{a_{ij}}{k} = \sum_{k'} P(k'|k)\rho_{k'}, \tag{56}$$

where we have used the identity Eq. (22). For uncorrelated networks with $P(k'|k) = k'P(k')/\langle k\rangle$ and assuming that the dynamics at large times is in its asymptotic diffusion-limited regime (in finite networks) $\rho_k \sim k\rho/\langle k\rangle$, Eq. (36), the degree resolved correlation function in absence of dynamical correlations takes the form

$$\chi^0(t;k) = \chi^0 = \frac{\langle k^2\rangle}{\langle k\rangle^2}, \tag{57}$$

independent of time and degree, and being only a function of the degree fluctuations, which increases as γ decreases, in agreement with numerical simulations. However, the degree resolved correlation function shown in Fig. 5 is flat only for degrees larger than 10, whereas it decreases as the degree decreases. Besides, the whole curve is slightly smaller than the MF prediction (dashed line in Fig. 5). This is a direct consequence of fact that, even if the network is small-world, there are some dynamical correlations that try to place particles apart.

Density correlations can be extended to the case of the $A+B\to\emptyset$ process, –or to the more general process defined in Eq. (8)– in order to account for the lack of particle segregation [27, 25] in this RD systems. In this case, coupled correlation functions must be defined, starting from the quantity $\rho^{\alpha,\beta}_{nn}(t;k)$, defined as the average density of particles of type β at the nearest neighbors of vertices of degree k filled with α particles ($\alpha,\beta = A,B$), namely,

$$\rho_{nn}^{\alpha,\beta}(t;k) = \frac{1}{n_k^{\alpha}(t)} \left\langle \sum_{i \in \mathscr{V}(k)} n_i^{\alpha}(t) \sum_j \frac{a_{ij} n_j^{\beta}(t)}{k} \right\rangle, \tag{58}$$

the associated normalized density correlation function being given by

$$\chi^{\alpha,\beta}(t;k) = \frac{\rho_{nn}^{\alpha,\beta}(t;k)}{\rho^{\beta}(t)}. \tag{59}$$

3.3 Degree effects on annihilation

The evolution of the dynamics in SF networks is better understood by analyzing its resolution in degree. Indeed, the density of particles at any time t depends on the degree of the vertex. At the MF level, the expression of the density of particles at vertices of degree k, Eq. (36), for the $A+A \to \emptyset$ process ($\mu = 1$) takes the form, within the quasi-static approximation,

$$\rho_k(t) = \frac{k\rho(t)/\langle k \rangle}{1 + 2k\rho(t)/\langle k \rangle}, \tag{60}$$

which implies that high degree vertices host a constant density while low degree vertices host a density of particles proportional to their degree [26]. In particular, at any given time t the partial density of vertices with degree larger than $\langle k \rangle / 2\rho(t)$ is constant and equal to $1/2$ up to time t. As the dynamics evolves, the fraction of degrees associated to a constant density shrinks and more and more vertices acquire a density proportional to their degree. For large t, no vertex is left in the network with degree larger than $\langle k \rangle / 2\rho(t)$. Therefore, when the density of particles satisfies $\rho(t) << \langle k \rangle / 2k_c$ (being k_c the maximum degree of the network), then $\rho_k(t) \sim k$ in all degree range. Simulations confirm this picture, as reported by the plots of the particle density at vertices of degree k for snapshots of the dynamics at various times, Fig.6(top). We can further check the validity of Eq. (60) by noticing that, if it

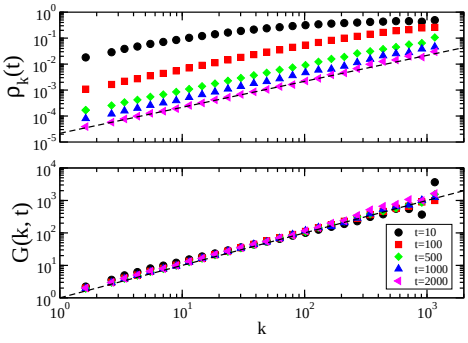

Fig. 6 Degree dependence of $A+A \to \emptyset$ dynamics on uncorrelated SF networks with degree exponent $\gamma = 3$ and size $N = 10^5$. Top: Particle density at vertices of degree k at different time snapshots. Bottom: data collapse of the partial densities according to Eq. (61). The dashed line represents a linear trend.

holds, then the function

$$G(k,t) = \frac{\langle k \rangle \rho_k(t)}{\rho(t)[1-2\rho_k(t)]} \tag{61}$$

should satisfy $G(k,t) = k$, independently of t. This is confirmed in Fig. 6(bottom), where we find a perfect collapse for widely separated time snapshots.

To understand this behavior, one has to consider that high degree vertices are likely to have some of their numerous nearest neighbors occupied by particles, given the correlated nature of the process (see section 4). Thus, in the high density regime, high degree vertices are always surrounded by a large number of occupied nearest neighbors. Eventually, one of these nearby particles will diffuse into a hub, annihilating the particle in it, if there was one, or filling the hub, if it was empty. This implies that during this phase of the dynamics, hubs spend half of their time occupied and the other half empty, explaining why, on average, the concentration is $1/2$. In other words, hubs act as drains through which particles vanish while their density is steadily maintained constant by a continuous replacing of nearby particles [26]. The absence of such replacing mechanism implies the decrease of the partial density of low degree vertices. However, as the global density decrease, the replacing mechanism gets more and more restricted to a shrinking fraction of very high degree vertices. In the end, the mechanism disappears and the only factor determining the density becomes the probability of being visited by a diffusing particle. Thus, the density gets proportional to the degree, $\rho_k(t) \sim k\rho(t)/\langle k \rangle$, similarly to what happens in a pure random walk [32].

This picture is further confirmed by the analysis of the annihilation rates at vertices of different degrees [51]. Let $m_t(k)$ be the probability that an annihilation event takes place in a single vertex of degree k during the interval t and $t+dt$. At the MF level, this rate corresponds to the annihilation term in Eq. (23)

$$m_t(k) = 2\rho_k(t) \sum_{k'} \frac{kP(k'|k)}{k'} \rho_{k'}(t), \tag{62}$$

that, in the uncorrelated case, reads

$$m_t(k) = \frac{2k\rho_k(t)\rho(t)}{\langle k \rangle}. \tag{63}$$

Therefore, the probability per unit of time of an annihilation event in any vertex increases with the probability that it is occupied and with the number of links pointing to it. As a consequence, for large degrees and moderate times, such that $\rho_k(t) \sim 1/2$, we have $m_t(k) \sim k$, while for small degrees, for which $\rho_k(t) \sim k$, we expect the behavior $m_t(k) \sim k^2$. This picture in confirmed by the numerical simulations reported in Fig. 7 for different snapshots of the dynamics. To compute $m_t(k)$ numerically, we first compute the quantity $M_t(k)$, defined as the annihilation rate for the class of degree k. This new quantity is computed as the ratio between the number of annihilation events happening at vertices of degree k and the total number of annihilation

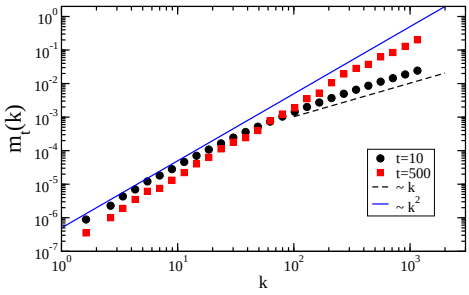

Fig. 7 Probability per unit of time that an annihilation event takes place in a vertex of degree k, $m_t(k)$, at different time snapshots, for the $A+A \to \emptyset$ dynamics on uncorrelated SF networks with degree exponent $\gamma = 3$ and size $N = 10^5$.

events during the interval $[t, t+\delta t]$, for δt small. Finally, the annihilation rate at single vertices is computed as $m_t(k) = M_t(k)/(\delta t N P(k))$. We consider the time interval $\delta t = 10$.

3.4 Effects of the minimum degree of the network

The MF predictions presented in Section 2 refer to generic uncorrelated SF networks. In all these results, the role of the minimum degree of the network, m, turns out to be irrelevant. It has been claimed, however, that dynamics performed in networks with $m = 1$ deviate from the theoretically predicted behavior, which is only recovered for $m > 1$ [38]. In Ref. [38] this deviation is attributed to some property of the topology related to the presence of dead ends in the network.

However, the observed deviations can be simply understood by considering that the dynamics is performed in this case on an effective topology with anomalies in the degree distribution and correlation spectrum. Indeed, it is impossible to generate SF networks both uncorrelated and globally connected when the minimum degree is $m = 1$ [35, 52]. In this case, a SF network always breaks up into a set of disconnected components –unless we introduce some correlations in order to avoid it. Therefore, the dynamics must be performed on the giant connected component (GCC) [34] of the resulting network, which has a topological structure that deviates from that of the total graph. Fig. 8 shows this effect. The degree distribution for low degrees of the GCC does not match the one for the whole network, Fig. 8(top). Besides, degree-degree correlations emerge in the GCC at the same range of degrees, Fig. 8(bottom), detected in this case by the average degree of the nearest neighbors of vertices of degree k, $\bar{k}_{nn}(k)$ [28]. The consequence of this change in the topology of the graph is a slowing down of the initial part of the dynamics. This can be seen in Fig. 9, where we plot the inverse of the particle density as a function of time for SF networks generated with the UCM algorithm with $m = 1$ and $m = 2$.

A deeper insight is gained by looking at the degree resolution of the density, Fig. 9(inset). While in a connected ($m > 1$) network, low degree vertices immediately acquire a density proportional to their degree (see Sec. 3.3), this process is much slower on the GCC of a network with $m = 1$, where low degrees exhibit de-

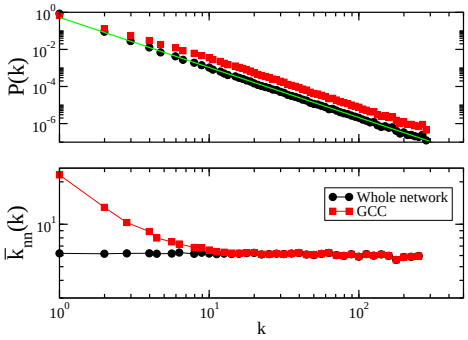

Fig. 8 Degree distribution (top) and correlations (bottom) for a UCM networks with $\gamma = 2.7$, $m = 1$, and size $N = 10^5$ The difference between the topology of the whole network and the GCC affects low degree vertices, where the GCC distribution deviates from the theoretical one and correlations appear.

viations from the expected degree distribution and correlations. Nevertheless, the global dynamics is dominated in the long term by high degree vertices, whose degree distribution and correlations are coherent with the expected ones. This explains why the density displays for long times the expected linear trend. Moreover, one can see that, after a transient period, the degree resolution of the density behaves as predicted by the MF theory.

3.5 Effects of a tree topology

Substantial deviations from the theoretically predicted trends in RD processes are observed when the dynamics is performed on networks with $m = 1$ and absence of loops, i.e. on trees [53], deviations that also show up in other dynamical systems [54, 55]. In this case, the process experiences a slowing-down and never reaches the asymptotic linear trend that dominates the dynamics in looped networks.

While the UCM model generates looped networks with arbitrary degree distributions[3], in the case of loopless networks we have only available the Barabasi-Albert

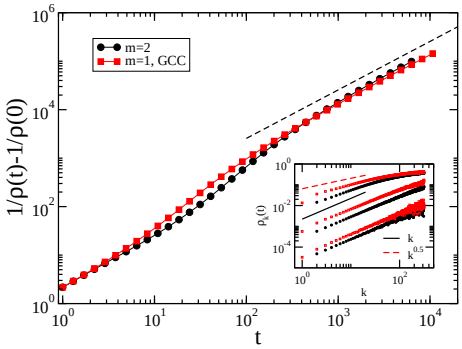

Fig. 9 Density of surviving particles in SF networks with $\gamma = 2.5$, $N = 10^5$, generated with the UCM algorithm for $m = 1$ (restricted to the GCC) and $m = 2$. Inset: degree resolution of the density at times $t = 10, 100$ and 1000 (from up to down).

[3] The length of these loops is, however, of the order $\log N$.

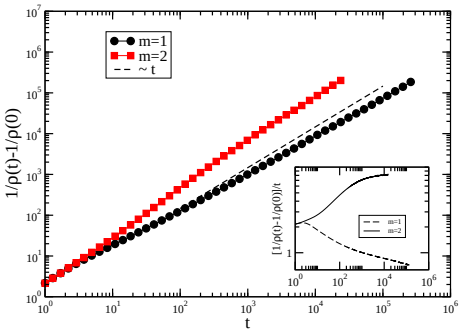

Fig. 10 Density of surviving particles in a tree structured and looped network: BA networks with size $N = 10^6$ and minimum degree $m = 1, 2$. The dashed line represents the linear trend. Inset: plot the same quantity divided by t.

model (BA) [6] with $m = 1$ and $\gamma = 3$[4] Thus, we restrict our comparison to this value of the degree exponent. In Fig. 10, we compare results of numerical simulations of the diffusion annihilation process on uncorrelated SF networks with and without loops. The Figure shows that the dynamics on trees is systematically slowed down and never reaches a linear trend. A direct fit of the power law slope at long times yields the exponent $\alpha_T \sim 0.9$. The effective exponent smaller than 1 is further stressed in the inset of Fig. 10, where we plot the inverse density divided by t. This slowing down is a general feature of dynamical systems with a diffusive component, which can be related with the observed slowing down of simple diffusion (random walks) in tree networks [53, 58].

Interestingly, the degree dependence of the annihilation diffusion dynamics on trees is different from the looped networks case, as it was first noticed in Ref. [53]. In Fig. 11(top) one can see that the partial density in the hubs never reaches a linear trend and rather displays a sub-linear increase. This results in a kind of *depletion* of the trees' hubs, that impedes them to ever gain a density proportional to their degrees. The effects of high degree depletion are reflected as well in the probability $m_t(k)$ of an annihilation event in a vertex of degree k. The asymptotic quadratic trend observed in looped networks is never reached in trees, Fig. 11(bottom).

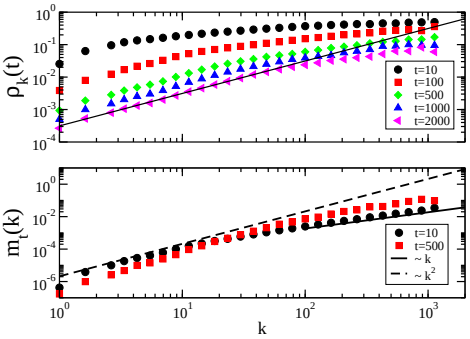

Fig. 11 Degree dependence of $A + A \to \emptyset$ dynamics on uncorrelated SF trees with degree exponent $\gamma = 3$ and size $N = 10^5$. Top: Particle density at vertices of degree k at different time snapshots. Bottom: Probability that an annihilation event takes place in a vertex of degree k at different time snapshots.

[4] Notice that the linear preferential attachment model [56] can generate tree networks with arbitrary γ, but intrinsically correlated except for $\gamma = 3$ [57].

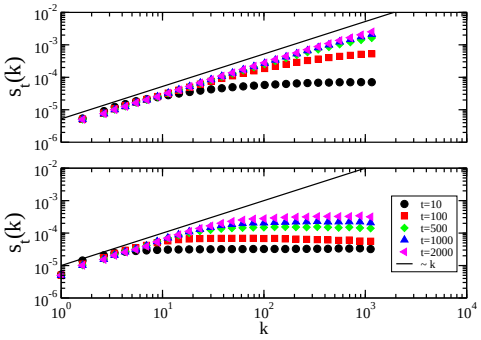

Fig. 12 Surviving occupation probability of $A+A \to \emptyset$ dynamics on uncorrelated SF with degree exponent $\gamma = 3$ and size $N = 10^5$ and different time snapshots. Top: results for looped networks ($m = 2$). Bottom: results for tree networks ($m = 1$).

An insight in the origin of this depletion is gained by measuring the occupation probability of a single site of degree k. We further restrict this measure by considering the surviving occupation probability of vertices of degree k at time t

$$s_t(k) = \frac{P_t^s(k)}{n(k)}, \tag{64}$$

where $P_t^s(k)$ is the occupation probability of degree class k at time t, computed including not all particles present at any $t' < t$, but only those that will survive until t, that is, that have performed a random walk of length t without ever encountering other particles. The results for this quantity as measured by simulations are reported in Fig. 12 for trees and looped uncorrelated networks with $\gamma = 3$. For any time t the ensemble of surviving particles is composed by those that have performed only diffusive steps until t, without experiencing any annihilation. However, the outcome of the simulations suggest that their random walk is biased. Indeed, $s_t(k)$ is strongly sublinear at high degrees, suggesting that the surviving random walks are those that have "avoided" high degree vertices. This is reasonable, since high degree vertices are those that host the higher density of particles and therefore falling on a high degree vertex almost surely implies for a walker to annihilate.

In reaction diffusion dynamics on looped networks this bias progressively disappear when the global density decreases, so that the particles surviving for large times end up exploring the network as pure random walkers. On the contrary, the bias is always present in tree structured networks.

4 Outlook

In this chapter we have reviewed the main results reported for reaction-diffusion processes on complex networks. As we have seen, many non-expected and interesting effects arise, as compared to regular lattices. More new results can be expected in the future, as both the analytical framework that has been developed and the nu-

merical techniques employed can be easily generalized to deal with different RD processes.

However, all the results and derivations presented so far correspond to a *fermionic* version of the RD dynamics, which suffers from two conceptual drawbacks: first, there is no systematic framework for the description of this kind of processes, and both numerical models and theoretical approximations (through heterogeneous MF theory) must be considered on a case by cases basis; and second, while it is relatively easy to deal with RD processes with reactions of order 2 (involving at most two particles), it becomes more problematic to implement reactions among three or more particles. Some attempts have been made in this direction. For example, in Ref. [59] the three-species process $A+B+C \to \emptyset$ was considered. However, to implement it within a fermionic formalism, the authors of [59] had to consider the presence of "intermediate" particles, produced by the reaction of two of the species, that afterwards can react with the third species to produce an actual annihilation event.

These type of multi-body interactions can be easily accounted for in a more general *bosonic* version of the dynamics, in which more than one particle are allowed to occupy a single vertex simultaneously. In this framework, reactions take place inside the vertices, with no restrictions regarding their order, and the interaction between vertices is mediated exclusively by diffusion. While some preliminary interesting work has been done in this direction [60, 61, 62], the full possibilities that the bosonic approach offers to the investigation of RD processes remain to be explored.

Acknowledgments

We thank M. Ángeles Serrano for a careful reading of the manuscript. M. B. acknowledges financial support from DGES, Grant FIS2007-66485-C02-02 and Generalitat de Catalunya Grant No. SGR00889. R.P.-S. acknowledges financial support from the Spanish MEC FEDER under Project No. FIS2007-66485-C02-01. M. C. acknowledges financial support from Universitat Politècnica de Catalunya.

References

1. R. Albert, A.L. Barabási, Rev. Mod. Phys. **74**, 47 (2002)
2. S.N. Dorogovtsev, J.F.F. Mendes, *Evolution of networks: From biological nets to the Internet and WWW* (Oxford University Press, Oxford, 2003)
3. M.E.J. Newman, SIAM Review **45**, 167 (2003)
4. B. Bollobás, *Modern Graph Theory* (Springer-Verlag, New York, 1998)
5. D.J. Watts, S.H. Strogatz, Nature **393**, 440 (1998)
6. A.L. Barabási, R. Albert, Science **286**, 509 (1999)
7. S. Dorogovtsev, A. Goltsev, J. Mendes. Critical phenomena in complex networks (2007). E-print arXiv:0705.0010v2 [cond-mat.stat-mech]
8. R. Pastor-Satorras, A. Vespignani, *Evolution and structure of the Internet: A statistical physics approach* (Cambridge University Press, Cambridge, 2004)

9. R.M. Anderson, R.M. May, *Infectious diseases in humans* (Oxford University Press, Oxford, 1992)
10. R. Cohen, K. Erez, D. ben Avraham, S. Havlin, Phys. Rev. Lett. **86**, 3682 (2001)
11. D.S. Callaway, M.E.J. Newman, S.H. Strogatz, D.J. Watts, Phys. Rev. Lett. **85**, 5468 (2000)
12. R. Pastor-Satorras, A. Vespignani, Phys. Rev. Lett. **86**, 3200 (2001)
13. A.L. Lloyd, R.M. May, Science **292**, 1316 (2001)
14. N.G. van Kampen, *Stochastic processes in chemistry and physics* (North Holland, Amsterdam, 1981)
15. J. Marro, R. Dickman, *Nonequilibrium phase transitions in lattice models* (Cambridge University Press, Cambridge, 1999)
16. O. Diekmann, J. Heesterbeek, *Mathematical epidemiology of infectious diseases: model building, analysis and interpretation* (John Wiley & Sons, New York, 2000)
17. J.D. Murray, *Mathematical biology*, 2nd edn. (Springer Verlag, Berlin, 1993)
18. M. Doi, J. Phys. A: Math. Gen. **9**, 1465 (1976)
19. M. Doi, J. Phys. A: Math. Gen. **9**, 1479 (1976)
20. L. Peliti, J. Phys. I **46**, 1469 (1985)
21. D.C. Mattis, M.L. Glasser, Rev. Mod. Phys. **70**, 979 (1998)
22. M. Le Bellac, *Quantum and statistical field theory* (Clarendon Press, Oxford, 1991)
23. A.A. Ovchinnikov, Y.B. Zeldovich, Chem. Phys. **28**, 215 (1978)
24. B.P. Lee, J. Phys. A: Math. Gen. **27**, 2633 (1994)
25. L.K. Gallos, P. Argyrakis, Phys. Rev. Lett. **92**, 138301 (2004)
26. M. Catanzaro, M. Boguñá, R. Pastor-Satorras, Phys. Rev. E **71**, 056104 (2005)
27. S. Weber, M. Porto, Phys. Rev. E **74**(4), 046108 (2006)
28. M.A. Serrano, M. Boguñá, R. Pastor-Satorras, A. Vespignani, in *Large scale structure and dynamics of complex networks: From information technology to finance and natural sciences*, ed. by G. Caldarelli, A. Vespignani (World Scientific, Singapore, 2007), pp. 35–66
29. R. Pastor-Satorras, A. Vespignani, Phys. Rev. E **63**, 066117 (2001)
30. M. Boguñá, R. Pastor-Satorras, A. Vespignani, in *Statistical Mechanics of Complex Networks*, *Lecture Notes in Physics*, vol. 625, ed. by R. Pastor-Satorras, J.M. Rubí, A. Díaz-Guilera (Springer Verlag, Berlin, 2003)
31. M. Boguñá, R. Pastor-Satorras, Phys. Rev. E **66**, 047104 (2002)
32. J.D. Noh, H. Rieger, Phys. Rev. Lett. **92**, 118701 (2004)
33. L. Lovász, in *Combinatorics, Paul Erdös is Eighty*, vol. 2, ed. by V.T.S. D. Miklós, T. Zsönyi (János Bolyai Mathematical Society, Bupadest, 1996), pp. 353–398
34. S.N. Dorogovtsev, J.F.F. Mendes, Adv. Phys. **51**, 1079 (2002)
35. M. Catanzaro, M. Boguñá, R. Pastor-Satorras, Phys. Rev. E **71**, 027103 (2005)
36. M. Boguñá, R. Pastor-Satorras, A. Vespignani, Euro. Phys. J. B **38**, 205 (2004)
37. M.E.J. Newman, in *Handbook of Graphs and Networks: From the Genome to the Internet*, ed. by S. Bornholdt, H.G. Schuster (Wiley-VCH, Berlin, 2003), pp. 35–68
38. L.K. Gallos, P. Argyrakis, Phys. Rev. E **72**, 017101 (2005)
39. M. Abramowitz, I.A. Stegun, *Handbook of mathematical functions.* (Dover, New York, 1972)
40. A. Bekessy, P. Bekessy, J. Komlos, Stud. Sci. Math. Hungar. **7**, 343 (1972)
41. E.A. Bender, E.R. Canfield, Journal of Combinatorial Theory A **24**, 296 (1978)
42. B. Bollobás, Eur. J. Comb. **1**, 311 (1980)
43. M. Molloy, B. Reed, Random Struct. Algorithms **6**, 161 (1995)
44. J. Park, M.E.J. Newman, Phys. Rev. E **66**, 026112 (2003)
45. S. Maslov, K. Sneppen, A. Zaliznyak, Physica A **333**, 529 (2004)
46. D. Torney, H. McConnell, J. Phys. Chem. **87**, 1441 (1983)
47. D. Torney, H. McConnell, Proc. R. Soc. Lond. A **387**, 147 (1983)
48. D. Toussaint, F. Wilczek, J. Chem. Phys. **78**, 2642 (1983)
49. L.K. Gallos, P. Argyrakis, J. Phys.: Condens. Matter **19**, 065123 (2007)
50. J. Newhouse, R. Kopelman, J. Phys. Chem. **92**, 1538 (1988)
51. L.K. Gallos, P. Argyrakis, Phys. Rev. E **74**, 056107 (2006)
52. R. Cohen, K. Erez, D. ben Avraham, S. Havlin, Phys. Rev. Lett. **85**, 4626 (2000)
53. J.D. Noh, S.W. Kim, Journal of the Korean Physical Society **48**, S202 (2006)

54. C. Castellano et al., Phys. Rev. E **71**, 066107 (2005)
55. L. Dall'Asta, A. Baronchelli, A. Barrat, V. Loreto, Phys. Rev. E **74**, 036105 (2006)
56. S.N. Dorogovtsev, J.F.F. Mendes, A.N. Samukhin, Phys. Rev. Lett. **85**, 4633 (2000)
57. A. Barrat, R. Pastor-Satorras, Phys. Rev. E **71**, 036127 (2005)
58. A. Baronchelli, M. Catanzaro, R. Pastor-Satorras. Random walks on scale-free trees (2008). E-print arXiv:0801.1278v1 [cond-mat.stat-mech]
59. K.H. Chang, K.G. Park, K.D. Ahan, S.Y. Kim, D.H. Ha, K. Kim, Journal of the Physical Society of Japan **76**, 035001 (2007)
60. V. Colizza, R. Pastor-Satorras, A. Vespignani, Nature Physics **3**, 276 (2007)
61. V. Colizza, A. Vespignani, Phys. Rev. Lett. **99**, 148701 (2007)
62. A. Baronchelli, M. Catanzaro, R. Pastor-Satorras. Bosonic reaction-diffusion processes on scale-free networks (2008). E-print arXiv:0802.3347v1 [cond-mat.stat-mech]

Index